Surface Science and Engineering 6(1387)91-104

Study of abrasive behavior for plasma electrolytic Oxidized Aluminum

M. Aliofkhazraei[1], M. Dadfar[2]and A. Sabour Rouhaghdam[1]

1. Faculty of Engineering, Materials Engineering Department, Tarbiat Modares University,
2. Faculty of Materials Engineering, Esfahan University of Technology, Esfahan, Iran

Abstract: Aluminum samples were coated by plasma electrolytic oxidation method to achieve 40µm of alumina oxide on their surface. Abrasive behavior with a rotating wheel-type apparatus has been examined with angular alumina and rounded silica abrasives as a function of test conditions, namely wheel-type rubber wheel or steel wheel and dry or wet environment conditions. Water tends to lubricate the contact between the particles and the sample, especially with small and/or rounded particles and thus the wear rate is reduced. With larger particles, the presence of water still affects wear, in that two-body abrasion may be favored, cutting enhanced and particle embedment reduced. The steel wheel tends to produce more fragmentation of abrasives, but in the wet environment, this is reduced as the lubricated contact with the sample results in lower stresses in the particles. The role of water has been shown to be significant in both the rubber and steel wheel tests and affects particle motion and particle fragmentation depending on particle type, shape and size and thus has a strong effect on wear rates and mechanisms observed. The conditions employed in a test used to simulate service conditions must be carefully chosen so as to mimic the latter conditions as closely as possible and the wet or dry environment is a significant parameter that must be considered.

Keywords*: Abrasive wear; Fragmentation; G105; Plasma electrolytic oxidation*
E-mail of corresponding author (s): *: maliofkh@gmail.com*

بررسی رفتار سایش خراشان آلومینیوم اکسید شده به روش پلاسمایی الکترولیتی

محمود علی‌اف خضرایی[۱]، مهدی دادفر[۲] و علیرضا صبور روح اقدم[۱]

۱ و ۲- بخش مهندسی مواد، دانشکده فنی و مهندسی، دانشگاه تربیت مدرس

۲- دانشکده مهندسی مواد، دانشگاه صنعتی اصفهان

چکیده

در این تحقیق نمونه‌های آلیاژ آلومینیوم ۶۰۸۲ توسط روش نسبتاً جدیدی به نام اکسیداسیون پلاسمایی الکترولیتی مورد عملیات اکسیداسیون قرار گرفتند و در نتیجه آن لایه‌ای از اکسید آلومینیوم فشرده با ضخامت ۴۰ میکرومتر بر روی سطح آنها تشکیل شد. سپس رفتار سایش خراشان این نمونه‌ها توسط دستگاه سایش خراشان ساخته شده تحت استاندارد ASTM G105، مورد بررسی قرار گرفت. پارامترهای مورد بررسی شامل نوع ذره ساینده (آلومینا و سیلیکا)، بار اعمالی، جنس چرخ دستگاه، اثر حضور آب به عنوان روان‌کننده و ... هستند. با توجه به نتایج به دست آمده، مشخص شد که در محیط خشک میزان خردایش ذرات ساینده بیشتر است درحالی که در محیط تر به علت وجود ماده روان‌کننده و کاهش تنش‌های موجود این میزان کمتر است. حضور آب در محیط، فارغ از جنس چرخ دستگاه، اثر به سزایی بر حرکت ذرات و خردایش آنها با توجه به نوع، شکل و اندازه ذره ساینده دارد و به همین جهت بر روی نرخ سایش و مکانیزم‌های آن بسیار تاثیرگذار است.

کلمات کلیدی : *آلومینیوم، استاندارد ASTM G105، اکسیداسیون پلاسمایی الکترولیتی، خردایش، سایش خراشان*

Introduction

Plasma electrolytic oxide (PEO) coatings [1-4] (sometimes referred to as micro-arc oxide coatings, or spark/discharge anodic coatings) are formed by substrate oxidation in an aqueous electrolyte via a series of localised electrical discharge events. These discharges allow oxide growth to proceed so as to produce films with thicknesses of the order of 100 μm. They are being explored and developed for various applications, including those for which wear resistance [5-10], corrosion resistance [7, 9, 11] and thermal protection [12-14] are being sought. Among the attractions of the process are that it involves very few health or safety hazards, and that coatings of uniform thickness can be quickly and easily produced on components with complex surface geometry, over a wide range of sizes.

However, much remains to be established before these coatings can be efficiently exploited and find widespread use. In particular, despite extensive study of the deposition process [15-18] and of coating microstructures [19-21], the mechanism of coating growth remains somewhat unclear, particularly in terms of the local physical processes occurring during growth. The present paper is focused on the abrasive properties exhibited by PEO coatings. Figures of the order of a few percent have commonly been quoted, with the assumption often made that this is largely associated with the deep pipe-like structures left by the most recent discharge events. However, there have been very few previous attempts at quantitative measurement of the wear resistance of PEO coatings. The present paper describes a systematic attempt to investigate its abrasive resistance under relative standards.

The most commonly used test configuration for three-body abrasion is that of a specimen loaded against a rotating wheel with abrasive particles being entrained into the contact zone. This is the basic principle of the tests encompassed in the ASTM standards G65 a dry sand–rubber wheel abrasion test, G105 a wet sand-rubber wheel abrasion test and B611 a wet sand-steel wheel abrasion test specifically for cemented carbides. All of these test types are predated by the Brinell abrasion testing machine that employed a rotating disk of open hearth iron and a stream of dry sand to abrade specimens.

2. Experimental method

Coatings were produced on BS 6082 aluminium alloy, in the form of a disc with 25 mm dia and 5 mm. Coatings were prepared using a 10 kW Keronite processing rig and a standard, commercially available electrolyte, consisting primarily of a dilute aqueous solution of KOH and Na_2SiO_4. The electrolyte was maintained at a temperature of approximately 25°C by re-circulation through a heat exchanger, with a whistle pump agitating and aerating the electrolyte. A constant capacitance condition was set, so as to achieve a current density of approximately 15 A dm^{-2} after the initial transitory regime. Coatings were grown to a thickness of approximately 40 μm. Thicknesses were measured using an Eban 2000 eddy current thickness gauge, the accuracy of which was confirmed by occasional microscopy of cross-sections.

A rotary wheel-type abrasive wear apparatus (see Fig. 1) that allows the use of abrasive either as dry particles or in aqueous slurry was employed to examine the abrasive wear behavior of plasma electrolytic oxidized BS 6082 aluminum samples. The dimensions of the disc shape specimens were 25 mm dia and 5 mm height. In this work, abrasive wear tests were performed with both rubber wheels and steel wheels. Details of the test apparatus can be found in ref [22]. Tests were performed under dry and wet conditions over a range of loads and abrasive types and sizes.

The abrasive particles used in this work were angular alumina and rounded silica. Three different size fractions (125-150, 355-425, and 500-600 μm) of each abrasive were

obtained by sieving. Abrasion tests were performed with alumina and silica abradents using both rubber and steel wheels under five loads in the range 23-75 N. The abrasive feed rates were kept constant as follows: all sizes of silica were fed at approximately 70 $g.min^{-1}$ and all sizes of alumina were fed at approximately 80 $g\ min^{-1}$ (the difference being due to different packing densities of the two materials). Wear rates were measured by specimen mass loss using a Sartorious CP324S electronic balance with an accuracy of 10^{-4} g. The wear rate quoted is the gradient of the mass loss data versus sliding distance taken from the steady state regime. All of the data were obtained by repeating experiments 4 times, averaging them and not considering out of range data

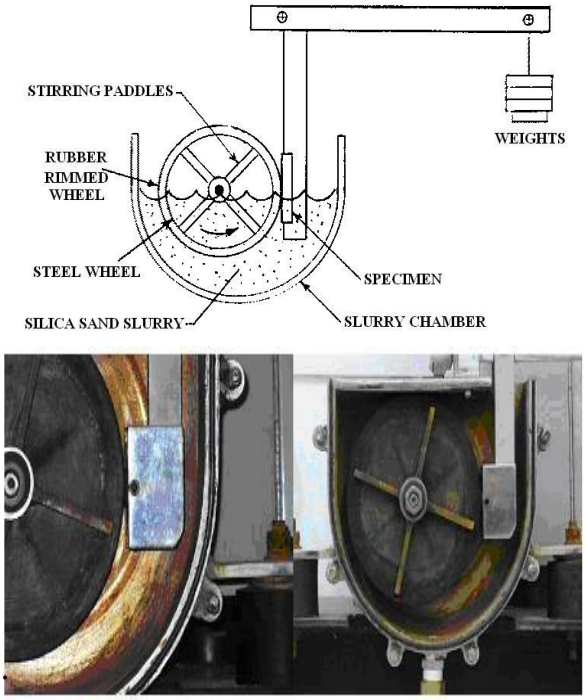

Fig. 1. Schematic diagram and pictures of abrasive wear test rig.

Fragmentation of abrasive particles during abrasion was determined by collecting abrasive particles following wear tests. Particles from the aqueous tests were sieved out from the slurry before drying. The used abrasive particles were then sieved into broad size fractions with the aid of a mechanical sieve shaker. Fragmentation was quantified as the percentage of material passing through the sieve with aperture approximately one half of the lower aperture size in the original fraction (i.e., that passing 180 μm for the 355-425 μm fractions and that passing 63 μm for the 125-150 μm fractions).

A Philips XL-30 scanning electron microscope was employed to reveal the morphology of the abrasive particles and the wear scars. Images were taken from the wear surfaces of the samples along the direction of abrasive movement. The hardness of the samples and abrasive particles were determined with a Buhler Micromet1 microhardness tester.

3. Results

Fig. 2 shows SEM micrographs of the medium (355-425 μm) sizes of each abrasive. All the alumina size fractions had similar angular morphologies, whereas the silica had a different shape depending on particle size. The two larger sizes, 355-425 and 500-600 μm, had a similar rounded shape, whereas the small size (125-150 μm) had more angular morphology; however, it was still less angular than the alumina particles. The alumina particles are harder than those of silica (Table 1).

Table 1
Hardnesses of the coated sample and the abrasive particles

Material	Hardness (HV200g)
Coated sample	~1700
Alumina abrasive	~2000
Silica abrasive	~1000

Rubber wheel and steel wheel abrasion tests of coated sample using both alumina and silica abrasives were performed in both dry and wet environments under a range of loads and with a range of abrasive particle sizes. An example of raw mass-loss data for one of the abrasive wear tests performed is shown in Fig. 3, demonstrating the linear increase in wear with sliding distance that was common in these tests. Fig. 4 shows an example of the steady state wear rate as a function of load. Such data has been plotted for each combination of

wheel type, abradent type, abradent size, and environment examined according to the simplified form of the Archard equation [23]:

$Q = kW$ (1)

where Q is the wear rate, k is the wear coefficient, and W is the applied load. Figs. 5 and 6 show the wear coefficient, k, for both types of wheel as a function of abrasive size and environment, for alumina and silica particles, respectively. It can be seen that the wear coefficient is a function of particle size and environment for all the wheel-environment combinations examined.

Scars on the coated sample following wear under a 75N load were examined by SEM. Fig. 7 shows surfaces through the wear scars produced by abrasion with a 355-425 µm alumina-rubber wheel combination under both dry and wet conditions. Figs. 8-10 show similar micrographs following abrasion by the 355-425 µm alumina-steel wheel combination, the 355-425 µm silica-rubber wheel combination, and the 355-425 µm silica-steel wheel combination, respectively.

Fragmentation of abradents initially in the size range 125-150 and 355-425 µm was measured following both wet and dry abrasion with both wheel types under a load of 75 N. Fig. 11 shows the degree of fragmentation for both the alumina and silica abradents as a function of particle size and test environment. Particle fragmentation is significant for both abrasive types in the dry-steel wheel test, but is significantly reduced by the presence of water. Fragmentation is significantly less in the rubber wheel tests than in the steel

Scars on the coated sample following wear under a 75N load were examined by SEM. Fig. 7 shows surfaces through the wear scars produced by abrasion with a 355-425 µm alumina-rubber wheel combination under both dry and wet conditions. Figs. 8-10 show similar micrographs following abrasion by the 355-425 µm alumina-steel wheel combination, the 355-425 µm silica-rubber wheel combination, and the 355-425 µm silica-steel wheel combination, respectively.

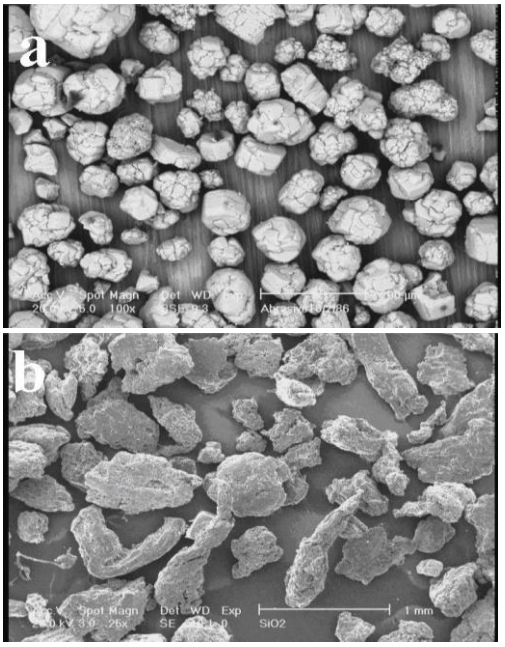

Fig. 2. Morphology of sieved particles: (a) alumina 355-425 µm and (b) silica 355-425 µm.

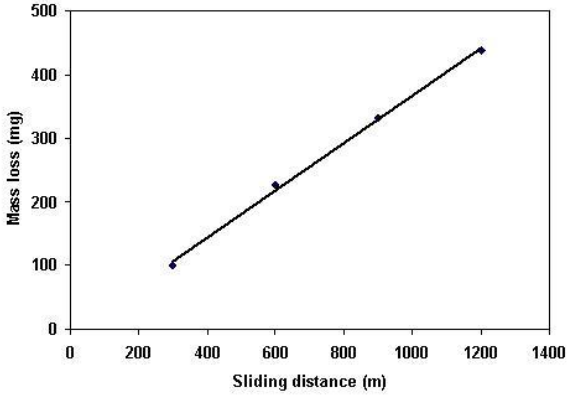

Fig. 3. Mass loss from coated sample as a function of sliding distance for rubber wheel dry abrasion with 125-150 µm silica under a 75N

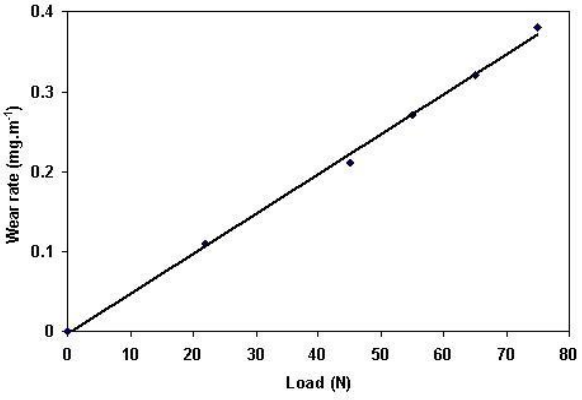

Fig. 4. Wear rate of coated sample abraded by dry 125-150 µm silica with the rubber wheel as a function of applied load.

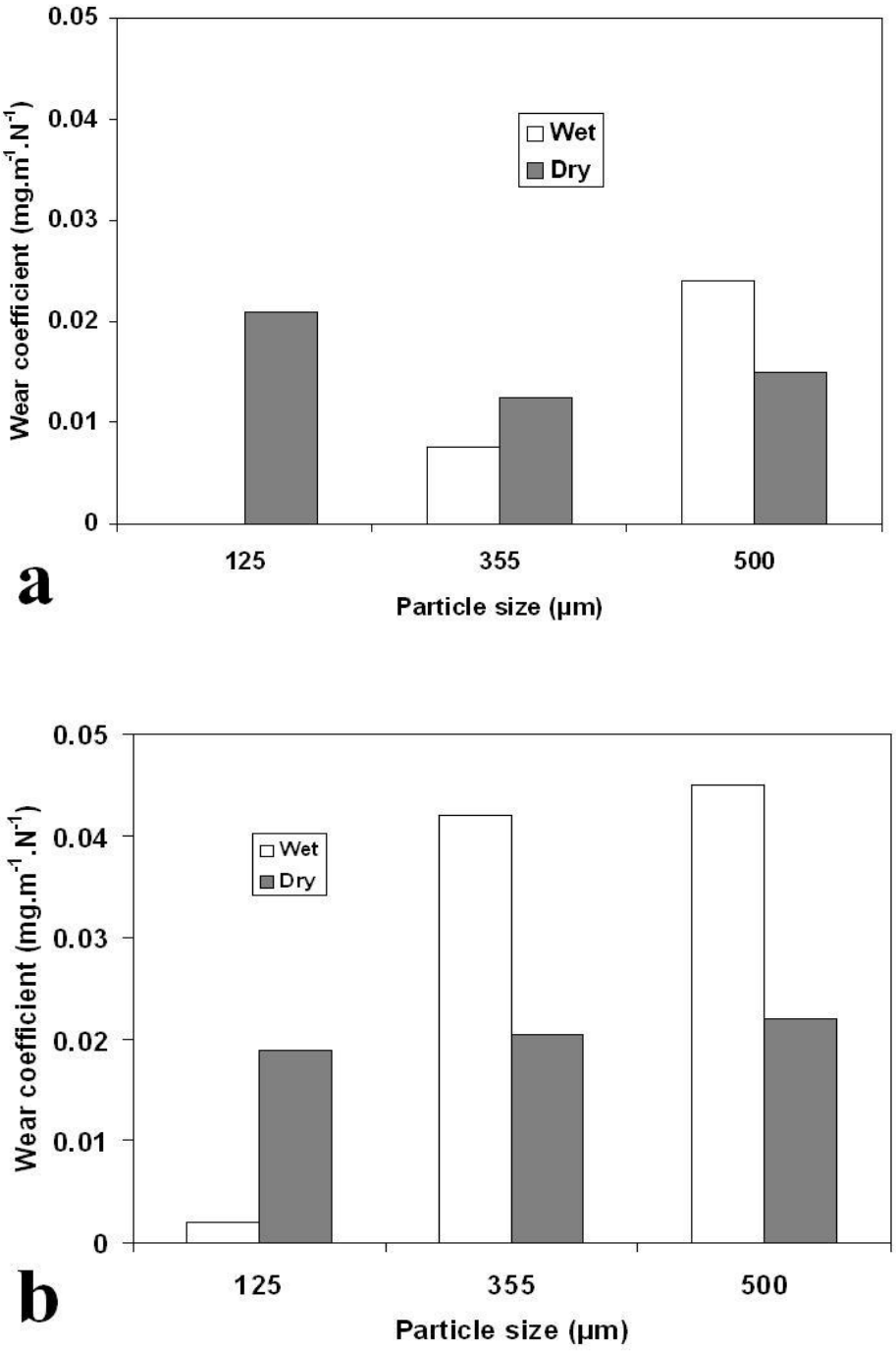

Fig. 5. Wear coefficient of coated sample following abrasive wear with alumina for both dry and wet environments as a function of abrasive particle size: (a) rubber wheel and (b) steel wheel.

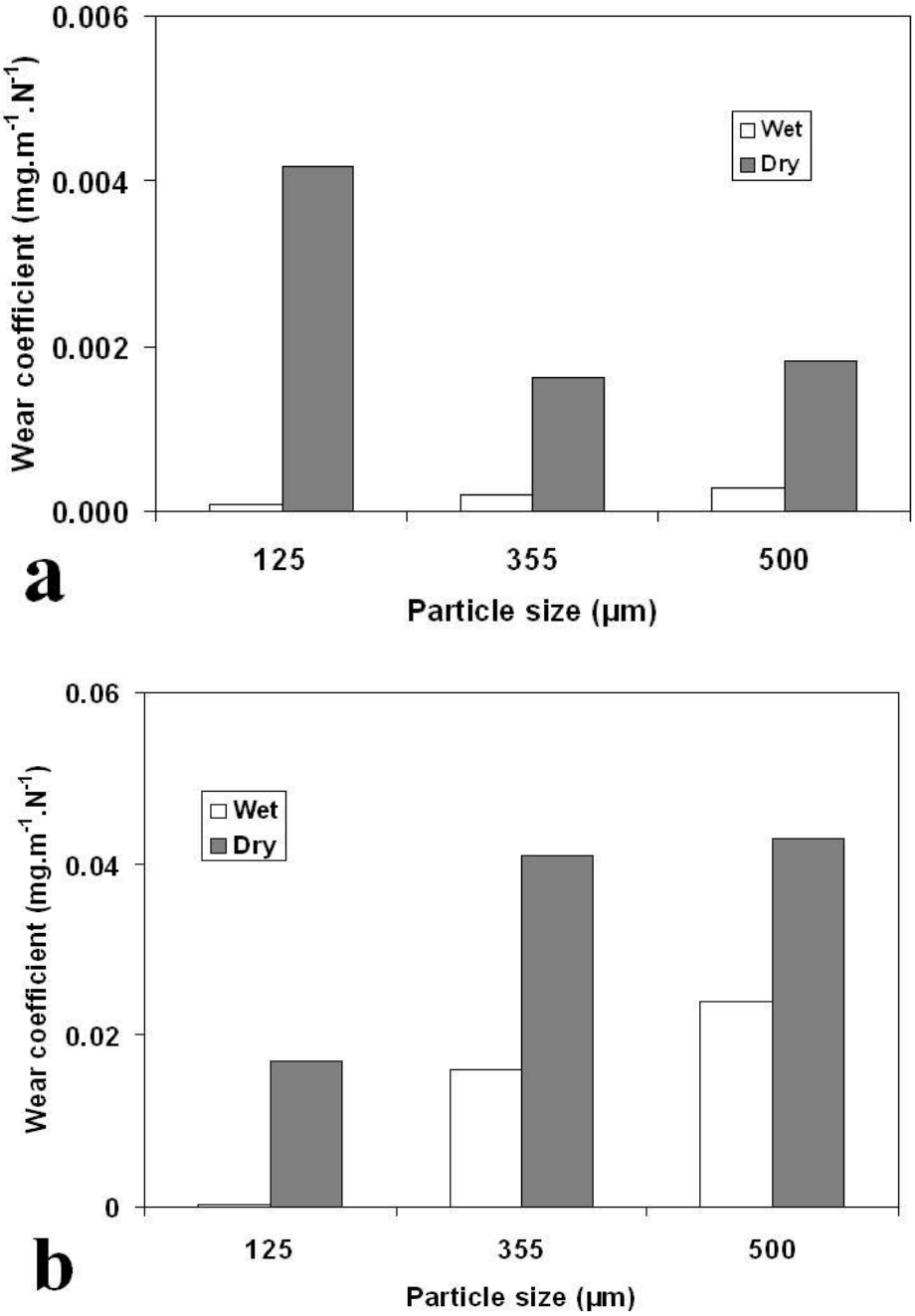

Fig. 6. Wear coefficient of coated sample following abrasive wear with silica (for both dry and wet environments) as a function of abrasive particle size: (a) rubber wheel and (b) steel wheel.

Scars on the coated sample following wear under a 75N load were examined by SEM. Fig. 7 shows surfaces through the wear scars produced by abrasion with a 355-425 µm alumina-rubber wheel combination under both dry and wet conditions. Figs. 8-10 show similar micrographs following abrasion by the 355-425 µm alumina-steel wheel combination, the 355 - 425 µm silica-rubber silica-steel wheel combination, respectively. Fragmentation of abradents initially in the size range 125-150 and 355-425 µm was measured following both wet and dry abrasion with both wheel types under a load of 75 N. Fig. 11 shows the degree of fragmentation for both the alumina and silica abradents as a function of particle size and test environment. Particle fragmentation is

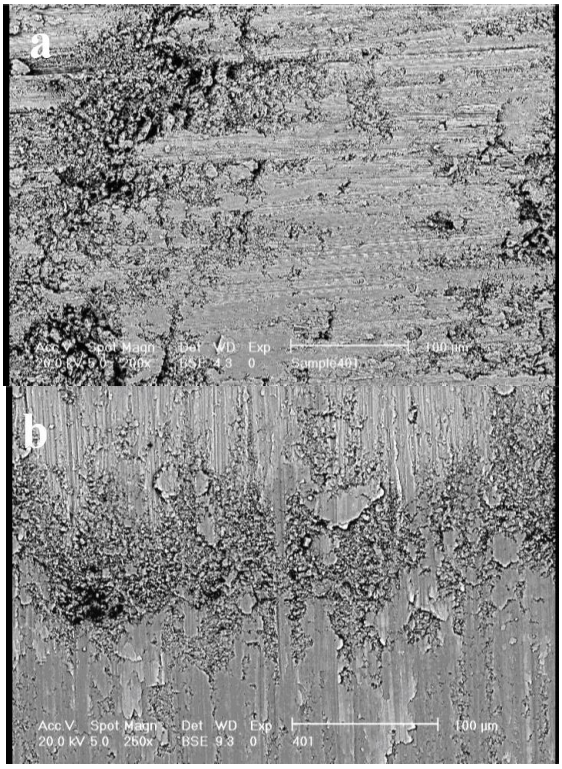

Fig. 7. SEM micrographs of surface of coated sample following abrasive wear with 355-425 µm alumina–rubber wheel as a function of environment: (a) dry-plan view (b) wet-plan view

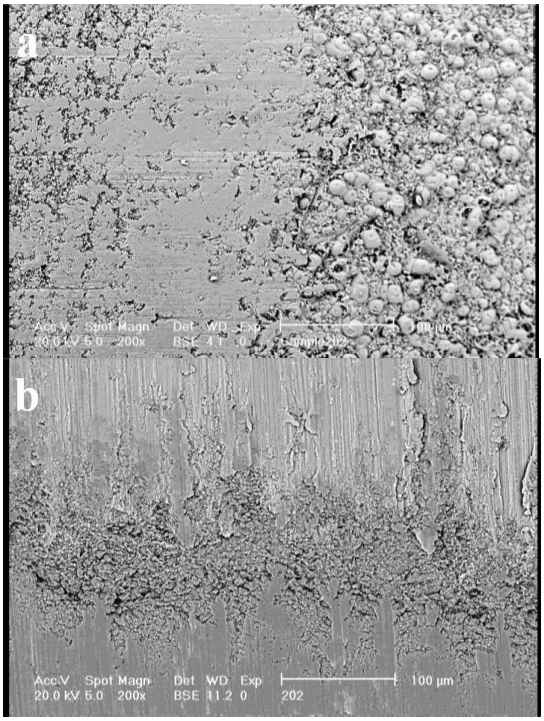

Fig. 8. SEM micrographs of surface of coated sample following abrasive wear with 355-425 µm alumina-steel wheel as a function of environment: (a) dry-plan view (b) wet-plan vie

significant for both abrasive types in the dry-steel wheel test, but is significantly reduced by the presence of water. Fragmentation is significantly less in the rubber wheel tests than in the steel Fragmentation of abradents initially in the size range 125-150 and 355-425 µm was measured following both wet and dry abrasion with both wheel types under a load of 75 N. Fig. 11 shows the degree of fragmentation for both the alumina and silica abradents as a function of particle size and test environment. Particle fragmentation is significant for both abrasive types in the dry-steel wheel test, but is significantly reduced by the presence of water. Fragmentation is significantly less in the rubber wheel tests than in the steel wheel tests. Fig. 12 shows SEM micrographs of the fractured abrasives initially 355-425 µm following dry abrasion testing with the steel wheel under a 75N load. Whilst fragmentation of the alumina is observed, its appearance is not significantly different to that of the virgin abrasive (Fig.2a) In contrast, the crushed silica shows significant particle size reduction and increased angularity when compared to the virgin silica (Fig. 2b).

4. Discussion

The abrasive wear rate of coated sample was generally directly proportional to load (as predicted by Eq. (1)) when abraded by both alumina and silica particles in both wet and dry environments with both rubber and steel wheels (for example, see Fig. 4). However, the wear coefficients, k, derived from such data show a marked dependence on the size and type of the abrading particles as well as the test environment. Microscopy has revealed significant changes in the mechanisms of wear in the different situations.

4.1. Wear by alumina with rubber and steel wheels

4.1.1. Rubber wheel

Under dry wear conditions with the alumina abradent-rubber wheel combination, the coated sample exhibited the highest wear coefficient (Fig. 5a) when abraded with the smallest particles 125-150 µm, with a value some 60% higher than those for abrasion with the two larger particle sizes which were similar in magnitude. This may be due to the angularity of particles increasing as their size decreases. In the wet environment, the wear coefficient was observed to rise rapidly with particle size (Fig.5a), with the wear coefficient for abrasion with 500-600 µm particles more than 100 times that for abrasion with 125-150 µm particles. Abrasion with the small particles is lubricated effectively by the water, but the lubrication becomes less effective as particle size increases. However, even when ineffective in preventing wear, the water does affect the motion of the particles in the abrasion zone. Fig. 7a shows a deeply indented and rough surface of the sample following dry abrasion whereas the surface following wet abrasion (Fig.7b) is much smoother whilst still exhibiting significant damage. In the wet environment, there is evidence of abrasive particle sliding across the surface (scratches parallel to the direction of particle motion) whereas in the dry condition, no sliding can be inferred from the micrograph, implying that particles roll and repeatedly indent the surface as they travel across it. Levels of abrasive particle fragmentation (Fig. 11) are low as expected in the rubber wheel test due to the compliance of the rubber limiting the forces exerted upon each particle.

4.1.2. Steel wheel

With the steel wheel, the dry wear coefficients were independent of particle size (Fig. 5b) and were of similar magnitude to those produced by rubber wheel abrasion. The wear scar Fig. 8a appears to have resulted from rolling indentation with a similarly roughened surface to that observed with rubber wheel abrasion (Fig. 7a).
However, embedment of the abrasive debris into the surface of the sample may also be

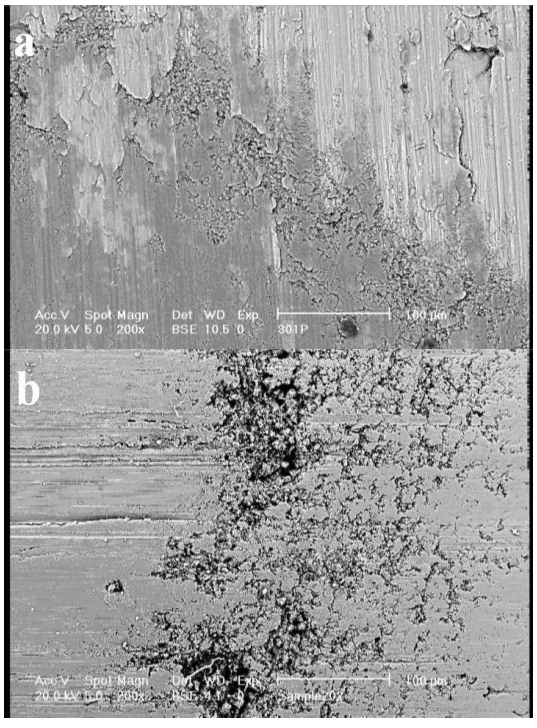

Fig. 9. SEM micrographs of surface of coated sample following abrasive wear with 355-425 µm silica–rubber wheel as a function of environment: (a) dry-plan view (b) wet-plan view.

Fig. 10. SEM micrographs of surface of coated sample following abrasive wear with 355-425 µm silica-steel wheel as a function of environment: (a) dry-plan view (b) wet-plan view

observed (Fig. 8b) that may subsequently act to reduce the observed wear rate by hardening the surface. Significant fracture of the alumina abrasive (~6% for the two particle sizes examined) has occurred implying that the stresses experienced (and thus the forces exerted) by the particles are higher in the steel wheel test than in the rubber wheel test. However, the effect of the higher forces in promoting wear has been countered by the effect of particle embedment into the coated sample increasing the wear resistance.

In the wet environment, the wear coefficient with the small alumina abrasive is again very small, indicating that the liquid was lubricating the contact between particle and sample effectively (Fig. 5b). As with the rubber wheel, lubrication was seen to become less effective as the particle size increased. Indeed, the wear rates in the aqueous environment were more than twice those observed under dry conditions for abrasion with 355 and 500 μm alumina.

The surface morphology (Fig. 8b) shows clean cutting, with no evidence for particle sliding such as long parallel scratches in the surface. As observed elsewhere [24], the water has washed the abrasive debris away from the surface and prevented its embedment. We may conclude that higher values of the wear coefficient in the wet environment are due to the efficacy of the lubricated cutting of the surface and the prevention of debris embedment in the surface of the sample. It has been commented that the tangential force on particles would be different in wet and dry conditions. It is notable that the fragmentation of both sizes of abradent examined is less in the wet environment than in the dry (Fig. 11) since the lubrication of the contact reduces the tangential traction forces on the particles. Furthermore, in the case where the lubrication of the particle-sample contact is effective in reducing the wear to almost zero (with 125-150 μm alumina abrasive), then the fragmentation of that abrasive is also reduced to almost zero.

4.2. Wear by silica with rubber and steel wheel

The wear coefficients for abrasion with silica with the rubber wheel in both dry and wet environments were significantly lower than those for abrasion with alumina. However, with the steel wheel, wear coefficients for abrasion with silica were of the same order of magnitude as those for abrasion with alumina. Patterns of behavior differ primarily due to differences in angularity and fracture strength of the two particle types.

4.2.1. Rubber wheel

In the dry environment with the rubber wheel, wear coefficients produced by abrasion with silica were lower than those for abrasion with alumina since the silica had a more rounded morphology (Fig. 2) which is less efficient for material removal. The wear coefficient for the 125-150 μm silica was higher than that of the two larger sizes (Fig. 6a) due to the smaller size having a significantly more angular shape than others. Wear scars for all sizes of silica showed similar morphologies and indicated wear by particles rolling across and indenting the surface and subsequent ductile fracture (Fig9a).

In the wet condition, wear coefficients were low for all sizes of particles (Fig. 6a). Wear scars were very smooth as seen from wear surfaces. Long parallel grooves are seen on the wear surface indicating that particles are sliding rather than rolling across the sample (two-body behavior rather than three-body behavior).

The particles will tend to orient themselves so that the tangential forces upon them are minimized, and thus the tendency to rotate is minimized. This will, in turn, lead to least damage of the sample and indicates that the water is lubricating the contact between the rounded abrasive and the surface effectively, resulting in very low levels of damage.

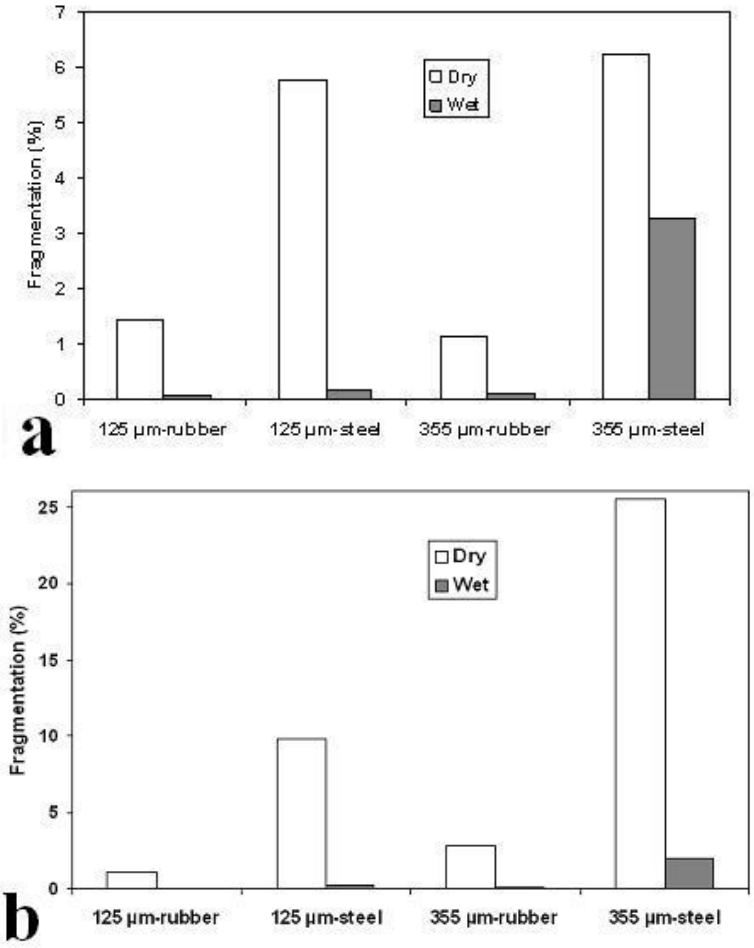

Fig. 11. Fragmentation of abradent particles following dry and wet abrasion tests with rubber and steel wheels under a load of 75 N as a function of initial particle size: (a) alumina and (b) silica.

The lubrication has altered the motion of the particle from a primarily rolling action in the dry environment to one of sliding in the wet environment. Fragmentation of the silica particles is low for abrasion in both wet and dry environments (Fig. 11) due to the low stresses on the particles in the rubber wheel tests.

4.2.2. Steel wheel

In abrasion tests with the steel wheel, wear coefficients were considerably higher than those with the rubber wheel in both dry and wet environments (Fig. 6).

In contrast to the rubber wheel test operated in dry conditions, use of the 125-150 µm silica abradent in the dry-steel wheel test resulted in a lower wear coefficient than use of the two larger sizes (Fig. 6b). Use of the steel wheel resulted in a significant degree of fragmentation of the silica abrasive. The fragmentation of the smaller silica was less severe (~10% fragmentation) than that of the larger silica (~26% fragmentation) under the same conditions (Fig. 11). This is due to the forces on each particle being smaller for the smaller particles (more particles in the contact zone at any time to support the load) along with the fact that small particles have generally been observed to exhibit higher fracture strengths than their larger counterparts. The newly fractured abrasive is highly angular (compare Fig. 12b with Fig. 2b) and thus is a highly efficient abradent. Thus, the lower degree of fragmentation of the smaller silica results in less wear of the

sample than with the larger silica. It is notable that the wear coefficients for abrasion with silica dry-steel wheel are higher than for abrasion with alumina under the same conditions. Again, comparison of Fig. 12a with b shows that the crushed silica is significantly more angular than the crushed alumina whilst Fig. 11 shows that the tendency for the silica to crush into highly abrasive particles is significantly greater than that for alumina. Wear with the in-situ fractured silica results in a heavily indented surface on the coated samples, again with no evidence of particles being dragged across it to produce scratches (Fig. 10a). It is also notable that the crushed silica does not embed into the sample as it did in the case of the alumina abrasive (compare Fig. 8b with Fig. 10b) and thus does not serve to reduce the wear rate.

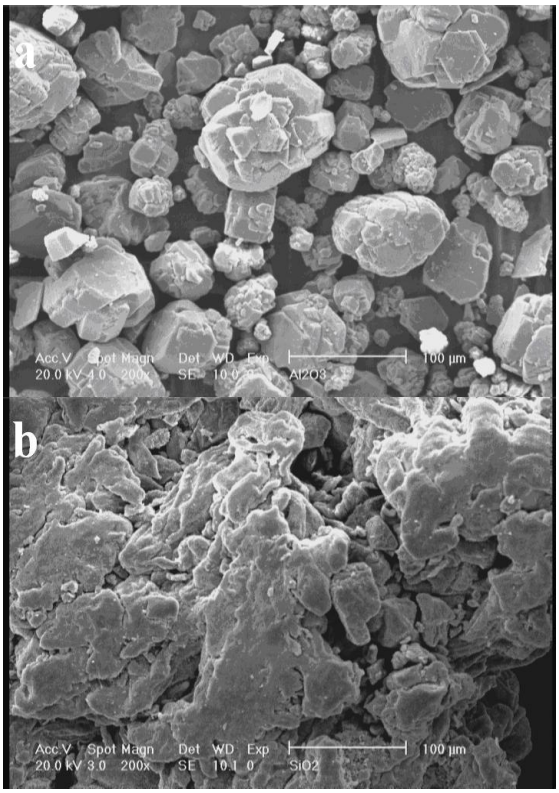

Fig. 12. SEM micrographs of debris of abrasive particles following dry-steel wheel abrasion test under a 75N load: (a) alumina 355-425 µm and (b) silica 355-425 µm.

In the wet environment, the wear coefficient increased with silica particle size and was lower than that in the dry condition. Most significantly, the fragmentation of the silica abrasive was dramatically reduced by the presence of water (Fig. 11). This reduction in fragmentation may result from a lowering of the tangential forces on the particles as a result of reduced friction, which reduces the maximum stresses in the particles below the fracture strength. Rounded particles are less prone to chipping than their angular counterparts since they have no stress concentrating corners or edges. The stresses will be further reduced if the particle slides across the surface (rather than rolling) in a two-body mode along a favorable (low stress) face due to its contact with the surface being lubricated (see Fig. 10b). The lack of fragmentation results in the morphology of the abrasive remaining rounded and thus abrasion with this rounded sand in the wet environment results in a significantly lower wear rate than that produced by the crushed sand in the dry condition. The wear scar (Fig. 10b) shows evidence for particles sliding across the surface as was observed for the rubber wheel in Fig. 9b along with some indentations, presumably resulting from the small fraction of fragmented particles.

5. Conclusions

It has been observed that the abrasive wear rate of plasma electrolytic oxidized aluminum sample is a function of abrasive type, size and test environment. In dry conditions, the wear rate with angular alumina abradent is similar with the rubber and steel wheels. However, the wear rate with silica abradent is far greater with a steel wheel than with a rubber wheel since, in the former case, the rounded silica is crushed to an angular form resulting in increased abrasivity. The small silica abradent is observed to crush less easily than the larger sizes and thus results in less wear. The larger sizes of silica that crushed easily in the steel wheel test resulted in wear rates even greater

than those observed with alumina abradent due to the high angularity and low tendency for embedment of the crushed silica.

Rates of abrasion were significantly altered by the presence of an aqueous carrier. In all cases, small particles produced low wear rates in water due to efficient lubrication of the particle-sample contact. Lowering of the tangential forces also resulted in the reduction of particle fragmentation. With angular alumina, the wear rate increased significantly as particle size increased, as the lubrication became ineffective with both rubber and steel wheels. The water prevented alumina abrasive particle embedment in the sample's surface as had been seen in the dry-steel wheel situation resulting in higher wear rates. With the silica abrasive, water was an effective lubricant for all particle sizes with the rubber wheel since the particles had a rounded morphology that was more easily lubricated. With the steel wheel, the water resulted in a significant reduction in fragmentation of the silica and wear was thus less than that in the dry environment.

In summary, we observed that:

1) Angular particles are more abrasive than rounded particles;

2) In-situ crushed particles are the most aggressive abradents;

3) The steel wheel in the dry condition produces particle fragmentation and, in the case of alumina, embedment of abrasive debris into the sample's surface;

4) Small and/or rounded particles can be well lubricated with water and thus result in low wear rates and low levels of fragmentation with both steel and rubber wheels;

5) The water environment reduced the tendency for abrasive particle embedment, and can result in effective lubrication which promotes particle sliding across the surface (two-body behavior) rather than particle rolling (three-body behavior). It also reduced the degree of abrasive particle fragmentation in all cases implying that the stresses on the particles have been reduced.

Acknowledgements

The coated samples for this research were prepared by Dr. J. Curran from Keronite international company (also from Cambridge University), many thanks to him. The authors would like to express their thanks to Arvandan Oil & Gas Production Company (TMU 85-09-66) and Iranian nano science and technology research organization for their support of the projects about plasma electrolysis.

References

1. Yerokhin A.L., Nie X., Leyland A., Matthews A., Dowey S.J., *Plasma electrolysis for surface engineering, Surface and Coatings Technology*, 122 (1999) 73-93.
2. X. Nie, A. Leyland, H.W. Song, A.L. Yerokhin, S.J. Dowey, A. Matthews, *Thickness effects on the mechanical properties of micro-arc discharge oxide coatings on aluminium alloys*, Surface and Coatings Technology, 119 (1999) 1055-60.
3. S.V. Gnedenkov, O.A. Khrisanfova, A.G. Zavidnaya, S.L. Sinebrukhov, P.S. Gordienko, S. Iwatsubo, A. Matsui, *Composition and adhesion of protective coatings on aluminum*, Surface and Coatings Technology, 145 (2001) 146-51.
4. J.A. Curran, T.W. *Clyne, Thermo-physical properties of plasma electrolytic oxide coatings on aluminium*, Surface and Coatings Technology, 199 (2005) 168-76.
5. A.A. Voevodin, A.L. Yerokhin, V.V. Lyubimov, M.S. Donley, J.S. Zabinski, *Characterization of wear protective Al-Si-O coatings formed on Al-based alloys by micro-arc discharge treatment*, Surface and Coatings Technology, 86-87 (1996) 516-21.
6. J. Tian, Z.Z. Luo, S.K. Qi, X.J. Sun, *Structure and antiwear behavior of micro-arc oxidized coatings on*

aluminum alloy, Surface and Coatings Technology, 154 (2002) 1-7.

7. X. Nie, E.I. Meletis, J.C. Jiang, A. Leyland, A.L. Yerokhin, A. Matthews, *Abrasive wear/corrosion properties and TEM analysis of Al_2O_3 coatings fabricated using plasma electrolysis*, Surface and Coatings Technology, 149 (2002) 245-51.
8. L. Rama-Krishna, K.R.C. Somaraju, G. Sundararajan, *The tribological performance of ultra-hard ceramic composite coatings obtained through microarc oxidation*, Surface and Coatings Technology, 163-164 (2003) 484-490.
9. M. Aliofkhazraei, P. Taheri, A. Sabour Rouhaghdam, Ch. Dehghanian, *Materials Science*, in press, will appear on No.3, 2007.
10. T. Wei, F. Yan, J. Tian, *Characterization and wear- and corrosion-resistance of microarc oxidation ceramic coatings on aluminum alloy*, Journal of Alloys Compound, 389 (2004) 169-76.
11. A.L. Yerokhin, X. Nie, A. Leyland, A. Matthews, *Characterisation of oxide films produced by plasma electrolytic oxidation of a Ti–6Al–4V alloy*, Surface and Coatings Technology, 130 (2000) 195-206.
12. P.I. Butyagin, Y.V. Khokhryakov, A.I. Mamaev, *Microplasma systems for creating coatings on aluminium alloys*, Material Letters, 57 (2003) 1748-51.
13. S.V. Gnedenkov, O.A. Khrisanfova, A.G. Zavidnaya, S.L. Sinebrukhov, A.N. Kovryanov, T.M. Scorobogatova, P. S. Gordienko, *Production of hard and heat-resistant coatings on aluminium using a plasma micro-discharge*, Surface and Coatings Technology, 123 (2000) 24-8.
14. J.A. Curran, T.W. Clyne, *The thermal conductivity of plasma electrolytic oxide coatings on aluminium and magnesium*, Surface and Coatings Technology, 199 (2005) 177-83.
15. A.L. Yerokhin, A.A. Voevodin, V.V. Lyubimov, J. Zabinski, M. Donley, *Plasma electrolytic fabrication of oxide ceramic surface layers for tribotechnical purposes on aluminium alloys*, Surface and Coatings Technology, 110 (1998) 140-6.
16. A.L. Yerokhin, A. Leyland, A. Matthews, *Kinetic aspects of aluminium titanate layer formation on titanium alloys by plasma electrolytic oxidation*, Applied Surface Science, 200 (2002) 172-84.
17. G. Sundararajan, L.R. Krishna, *Mechanisms underlying the formation of thick alumina coatings through the MAO coating technology*, Surface and Coatings Technology, 167 (2003) 269-77.
18. Y. Guangliang, L. Xianyi, B. Yizhen, C. Haifeng, J. Zengsun, The effe*cts of current density on the phase composition and microstructure properties of micro-arc oxidation coating*, Journal of Alloys Compound, 345 (2002) 196-200.
19. J. Chen, Y. Shi, L. Wang, F. Yan, F. Zhang, *Preparation and properties of hydroxyapatite-containing titania coating by* ***micro-arc oxidation,*** *Materials Letters*, 60 (20) (2006) 2538-2543.
20. W.B. Xue, C. Wang, R.Y. Chen, Z.W. Deng, *Structure and properties characterization of ceramic coatings produced on Ti–6Al–4V alloy by microarc oxidation in aluminate solution*, Material Letters, 52 (2002) 435-41.
21. Y. Han, S.H. Hong, K.W. Xu, *Structure and in vitro bioactivity of titania-based films by micro-arc oxidation*, Surface and Coatings Technology, 168 (2003) 249-58.

22. ASTM G105-89, *Standards test method for conducting wet sand/rubber wheel abrasion tests, ASTM Standards*.
23. G. Stachowiak, *Wear: Materials, Mechanisms and Practice*, John Wiley & Sons, ISBN 186058442X
24. J.B. Zu, G.T. Burstein, I.M. Hutchings, *A comparative study of the slurry erosion and free-fall particle erosion of aluminum*, Wear, 149 (1991) 73-84.